Supporting Information

Molecular mechanisms of resveratrol and EGCG in inhibition of $A\beta_{42}$ aggregation and disruption of $A\beta_{42}$ protofibril: similarities and differences

*Fangying Li, Chendi Zhan, Xuewei Dong and Guanghong Wei**

Department of Physics, State Key Laboratory of Surface Physics, Key Laboratory for Computational Physical Sciences (Ministry of Education), Fudan University, 2005 Songhu Road, Shanghai, 200438, People's Republic of China
*Corresponding author: Guanghong Wei, E-mail: ghwei@fudan.edu.cn

This material contains 20 supplemental figures.

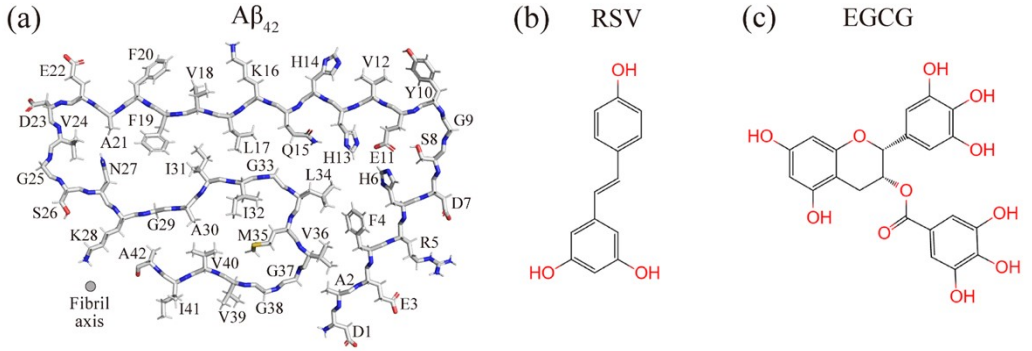

Figure S1. Structure illustration of (a) a single chain of an $A\beta_{42}$ protofibril, and the chemical structure of (b) a resveratrol (RSV) molecule and (c) an EGCG molecule.

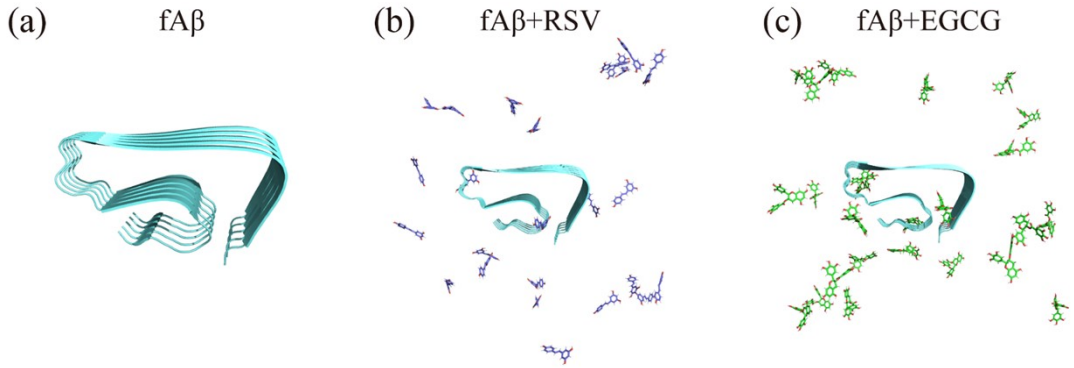

Figure S2. The initial structures of the full-length $A\beta_{42}$ pentameric protofibril in the absence and presence of RSV or EGCG. (a) The isolated $A\beta_{42}$ protofibril (fAβ system), (b) $A\beta_{42}$ protofibril with RSV molecules (fAβ+RSV system), and (c) $A\beta_{42}$ protofibril with EGCG molecules (fAβ+EGCG system). There are 25 RSV molecules in fAβ+RSV system and 25 EGCG molecules in fAβ+EGCG system. RSV or EGCG molecules were randomly placed around the $A\beta_{42}$ protofibril with a minimum distance of ~1.0 nm between RSV/EGCG and protofibril.

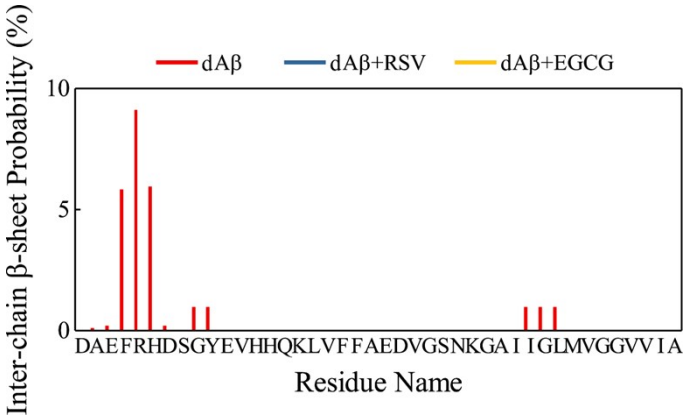

Figure S3. Residue-based inter-chain β-sheet probability in dAβ, dAβ+RSV, and dAβ+EGCG systems.

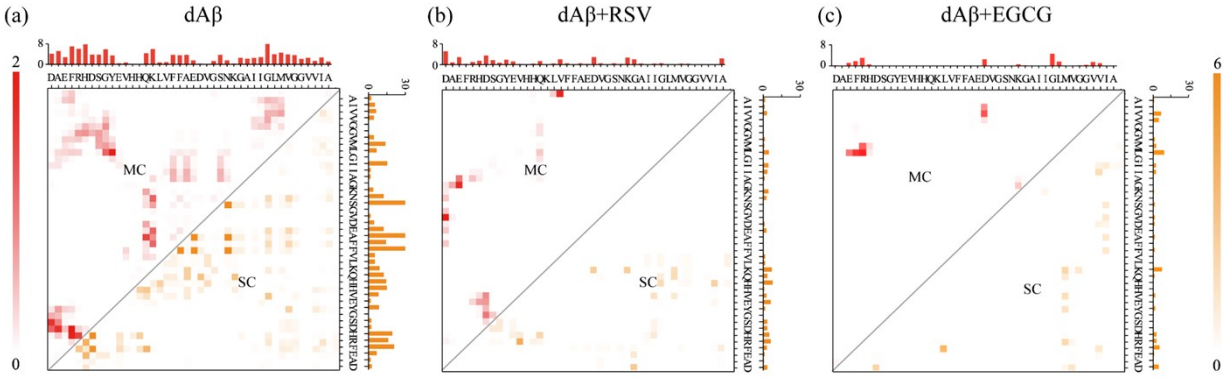

Figure S4. The effects of RSV and EGCG on the pairwise residue interactions between two $A\beta_{42}$ peptides. (a-c) Contact number map between two $A\beta_{42}$ peptides for the main-chain (MC) and side-chain (SC) atoms in the absence (a) or presence of RSV (b), and EGCG (c). The cumulative MC and SC contact numbers of each residue with all the other residues of $A\beta_{42}$ are shown respectively in the top and right of each panel.

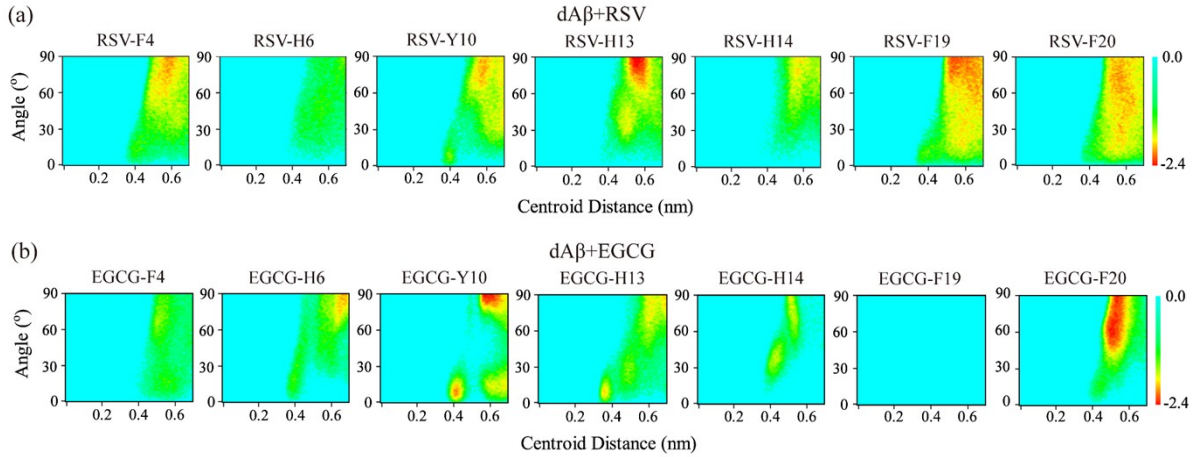

Figure S5. Potential mean force (PMF) (in kcal/mol) as a function of the centroid distance and the angle between one aromatic ring from (a) RSV or (b) EGCG and the other ring from aromatic residues in $A\beta_{42}$.

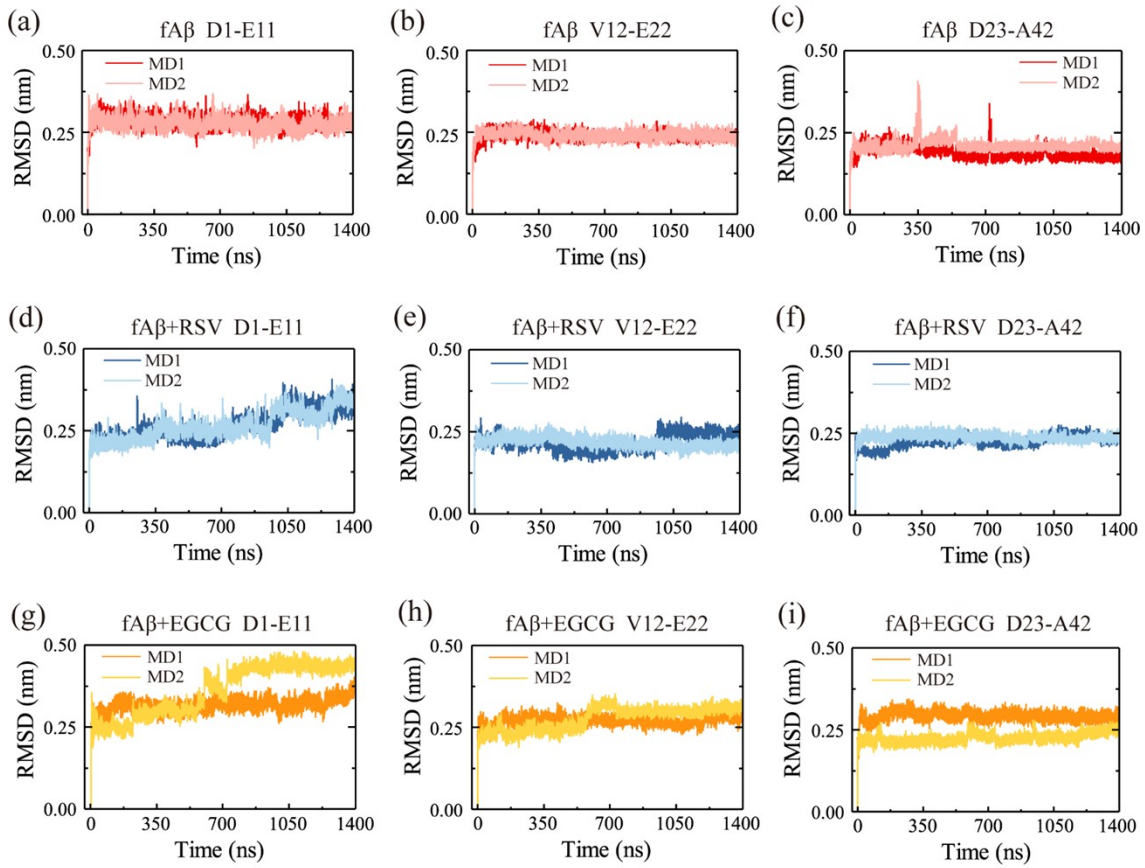

Figure S6. The time evolution of all-atom RMSD values of the D1-E11, V12-E22, and D23-A42 regions in (a-c) fAβ system, (d-f) fAβ+RSV system, and (g-i) fAβ+EGCG system.

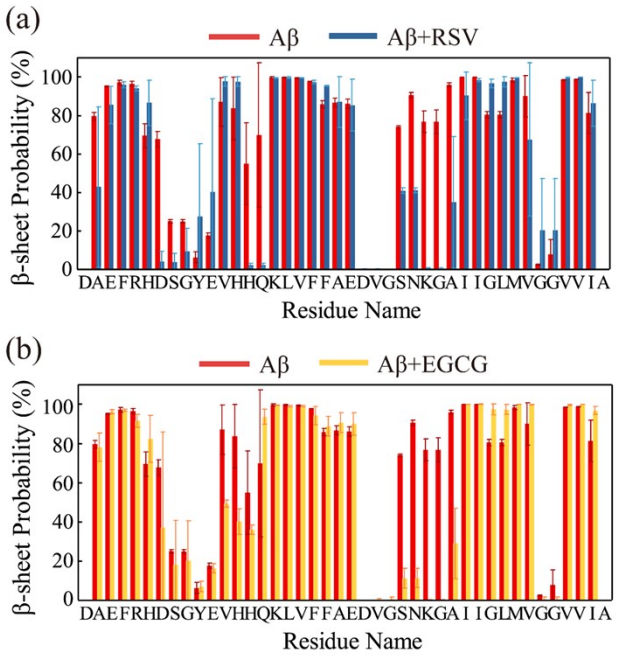

Figure S7. Residue-based β-sheet probability in (a) fAβ+RSV and (b) fAβ+EGCG systems. The error bars show the standard deviation over two simulations.

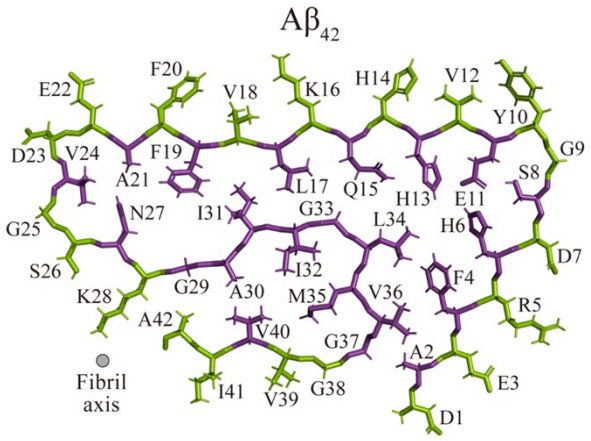

Figure S8. Structure illustration of a single chain of an $A\beta_{42}$ protofibril. Residues with side-chains facing outwards are colored in green, while residues with side-chains facing inwards are colored in purple.

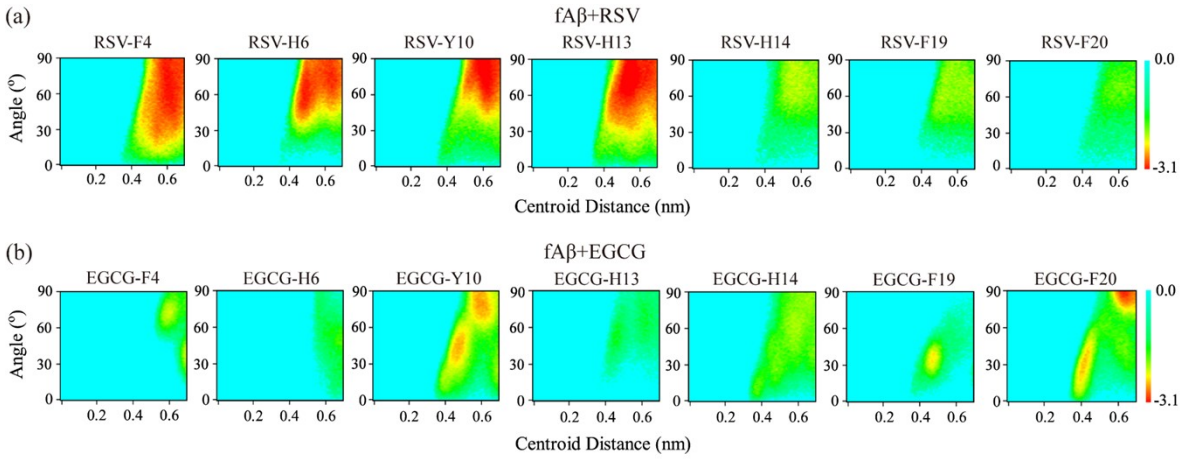

Figure S9. Potential mean force (PMF) (in kcal/mol) as a function of the centroid distance and the angle between one aromatic ring from (a) RSV or (b) EGCG and the other ring from aromatic residues in $A\beta_{42}$ protofibril.

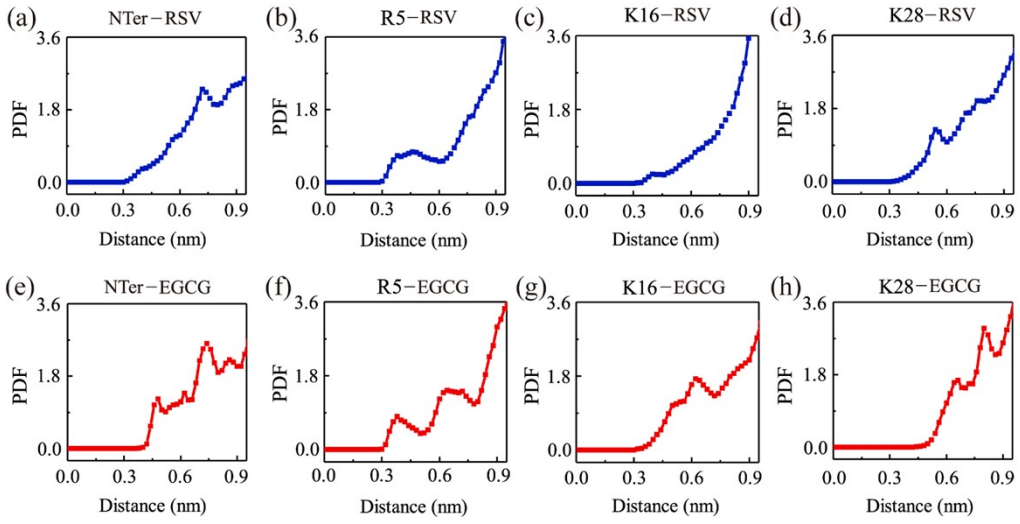

Figure S10. Cation-π interactions between RSV/EGCG molecules and $A\beta_{42}$ protofibril. Probability density function (PDF) as a function of the centroid distance of the sidechain NH_3^+ group from N-terminus residue D1, R5, K16, and K28 of the $A\beta_{42}$ peptide and an aromatic ring from (a-d) RSV and (e-h) EGCG.

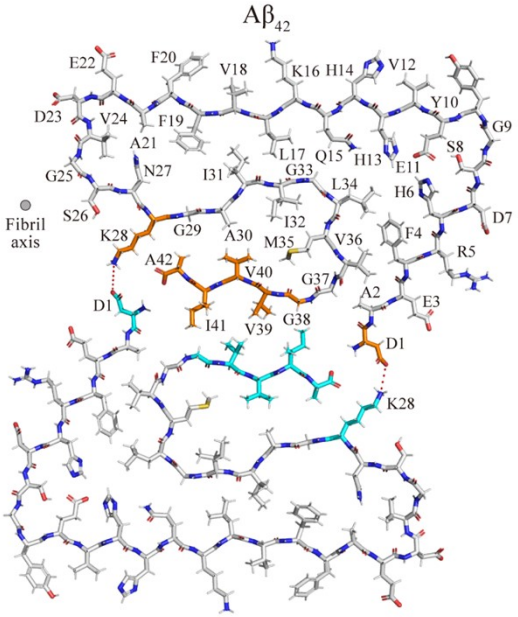

Figure S11. Structure illustration of a layer of an $A\beta_{42}$ fiber. The C-terminus residues G38, V39, V40, I41, A42, K28, and N-terminus residue D1 of two protofibrils are colored in orange and cyan, respectively. These residues form an interface for the association of protofibrils. D1-K28 salt bridges between two protofibrils are represented by red dash lines.

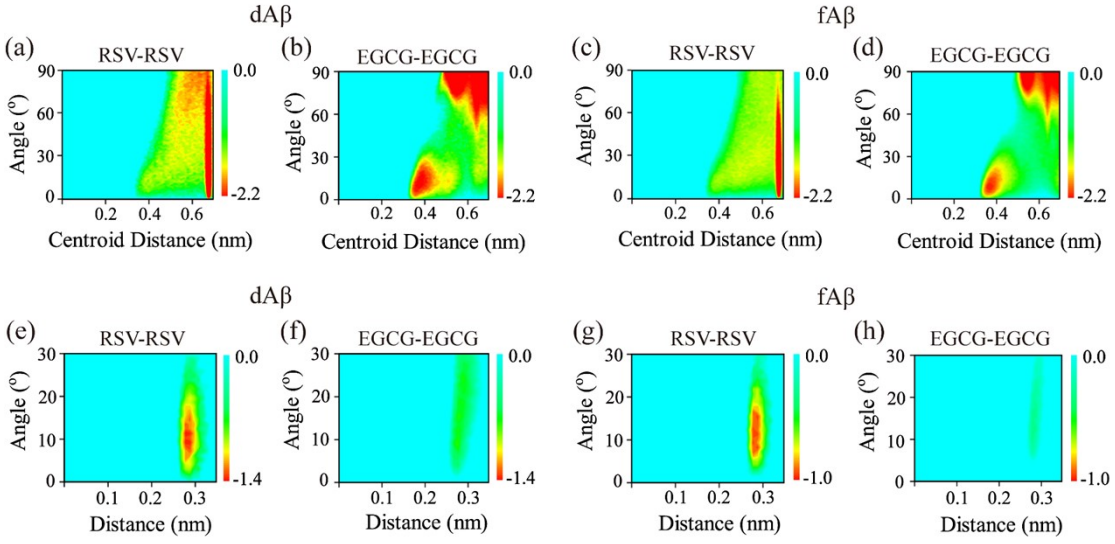

Figure S12. Comparison of π-π stacking interactions of RSV-RSV and EGCG-EGCG in $A\beta_{42}$ dimer (dAβ) and $A\beta_{42}$ protofibril (fAβ) systems. (a-d) PMF (in kcal/mol) as a function of the centroid distance and the angle between a pair of aromatic rings from RSV/EGCG in dAβ (a, b) and fAβ (c, d) systems. (e-h) PMF as a function of the distance between a hydrogen-bonding donor atom (D) and an acceptor atom (A) and the angle of D-H...A of RSV/EGCG in dAβ (e, f) and fAβ (g, h) systems.

Details of system setup and MD simulations of D23N mutant systems are given below:

D23N mutant $A\beta_{40}$ dimer with and without RSV or EGCG. The initial coordinates of the $A\beta_{40}$ monomer were taken from the solution NMR conformation of $A\beta_{40}$ (PDB ID: 2LFM).[1] By replacing Asp at site 23 with Asn in $A\beta_{40}$ monomer using pymol software, we constructed a D23N Iowa mutant (MT) $A\beta_{40}$ monomer. To mimic the neutral pH condition, the side-chains of Arg5, Lys16, Lys28, and the N-terminus were positively charged (NH_3^+), while the side-chains of Asp1, Glu3, Asp7, Glu11, Glu22, and the C-terminus were negatively charged (COO^-). In the initial state, two D23N $A\beta_{40}$ monomers were placed in parallel with a minimum distance of 1.2 nm.

Three systems were simulated (Fig. S13): the isolated mutant $A\beta_{40}$ dimer (MT-dAβ system), mutant $A\beta_{40}$ dimer with ten RSV molecules (MT-dAβ+RSV system), and mutant $A\beta_{40}$ dimer with ten EGCG (MT-dAβ+EGCG system). In both MT-dAβ+RSV and MT-dAβ+EGCG systems, RSV/EGCG molecules were randomly placed around the mutant $A\beta_{40}$ dimer with a minimum distance of ~1.0 nm.

D23N mutant $A\beta_{15\text{-}40}$ protofibril with and without RSV or EGCG. The initial coordinates of the mutant protofibrillar pentamer were taken from the solid state NMR derived D23N mutant $A\beta_{15\text{-}40}$ fibril (PDB ID: 2MPZ).[2] The initial structure of a single chain from the mutant protofibril is shown in Fig.S14. Three systems were simulated (Fig. S15): an isolated mutant $A\beta_{15\text{-}40}$ protofibril (MT-fAβ system), a mutant $A\beta_{15\text{-}40}$ protofibril in the presence of RSV molecules (MT-fAβ+RSV system), and a mutant $A\beta_{15\text{-}40}$ protofibril in the presence of EGCG molecules (MT-fAβ+EGCG system). In MT-fAβ+RSV and MT-fAβ+EGCG systems, there are respectively 25 resveratrol molecules and 25 EGCG molecules. RSV/EGCG molecules were randomly placed around the mutant $A\beta_{15\text{-}40}$ protofibril with a minimum distance of ~1.0 nm.

MD simulation details of D23N mutant systems. The D23N mutant $A\beta_{40}$ dimer and $A\beta_{15\text{-}40}$ protofibrils were placed in the center of a cubic box with a volume of 8.65×8.65×8.65 and 9.20×9.20×9.20 nm^3, respectively, filled with TIP3P water molecules. Na^+ or Cl^- ions were added to neutralize the electrostatic charges of the two systems, and additional NaCl was added to mimic a physiological salt concentration of 150 mM. The procedures of energy minimization, system equilibration, and production MD runs are the same as the WT $A\beta_{42}$ dimer and protofibril systems.

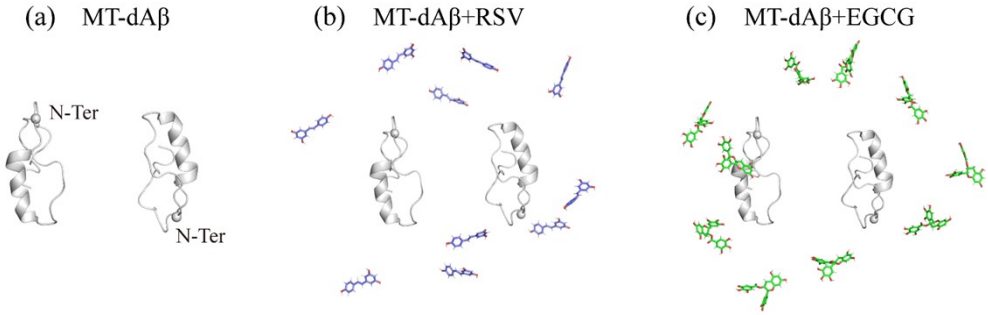

Figure S13. The initial states of D23N mutant $A\beta_{40}$ dimer systems: (a) the isolated MT $A\beta_{40}$ dimer (MT-dAβ system), (b) MT $A\beta_{40}$ dimer with RSV molecules (MT-dAβ+RSV system), and (c) MT $A\beta_{40}$ dimer with EGCG molecules (MT-dAβ+EGCG system).

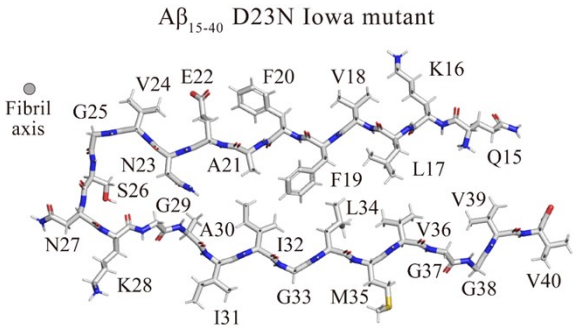

Figure S14. Structure illustration of a single chain of the D23N Iowa mutant $A\beta_{15-40}$ protofibril.

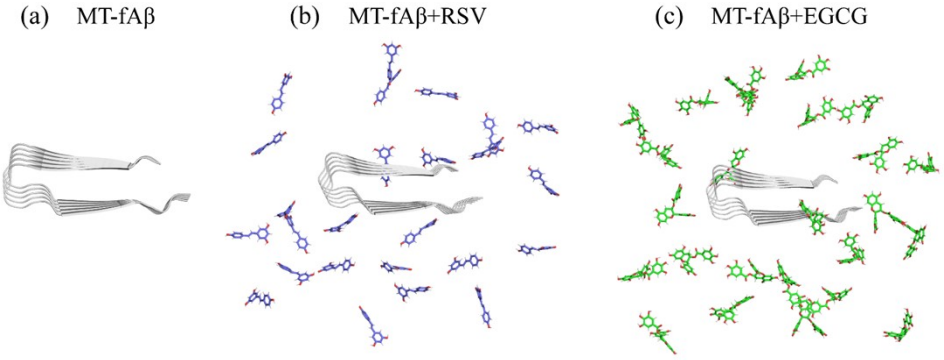

Figure S15. The initial states of the D23N mutant $A\beta_{15-40}$ protofibril systems: (a) The isolated MT $A\beta_{15-40}$ protofibril (MT-fAβ system), (b) MT $A\beta_{15-40}$ protofibril with RSV molecules (MT-fAβ+RSV system), and (c) MT $A\beta_{15-40}$ protofibril with EGCG molecules (MT-fAβ+EGCG system).

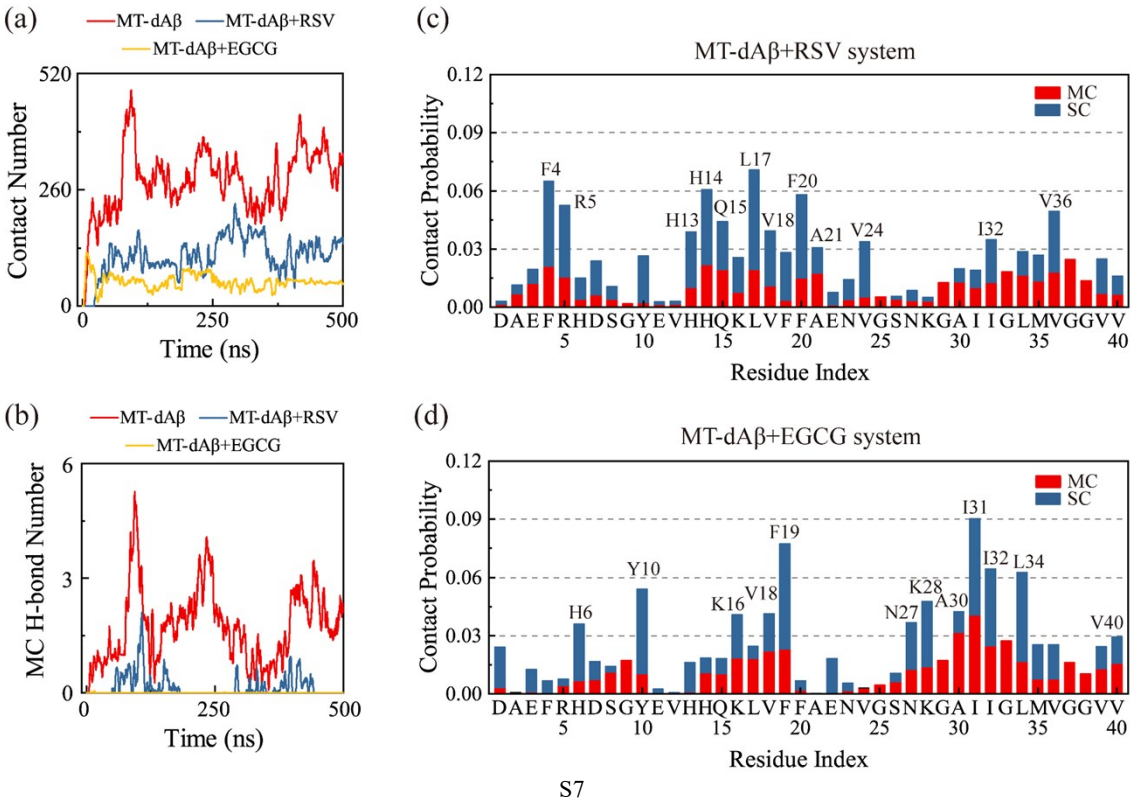

Figure S16. Inhibitory effect of RSV/EGCG on D23N MT $A\beta_{40}$ dimerization and binding site analysis. (a, b) The time evolution of the contact number (a) and MC hydrogen-bond number (b) between two MT $A\beta_{40}$ peptides in the absence or presence of RSV/EGCG. Data in (a, b) are smoothed using an adjacent-averaging method with a moving window of 50 points. (c, d) Analyses of binding sites between RSV/EGCG and MT $A\beta_{40}$ peptide. Contact probability between RSV (c) or EGCG (d) and the MC/SC atoms of each residue. Residues having relatively high contact probabilities with RSV or EGCG are labeled.

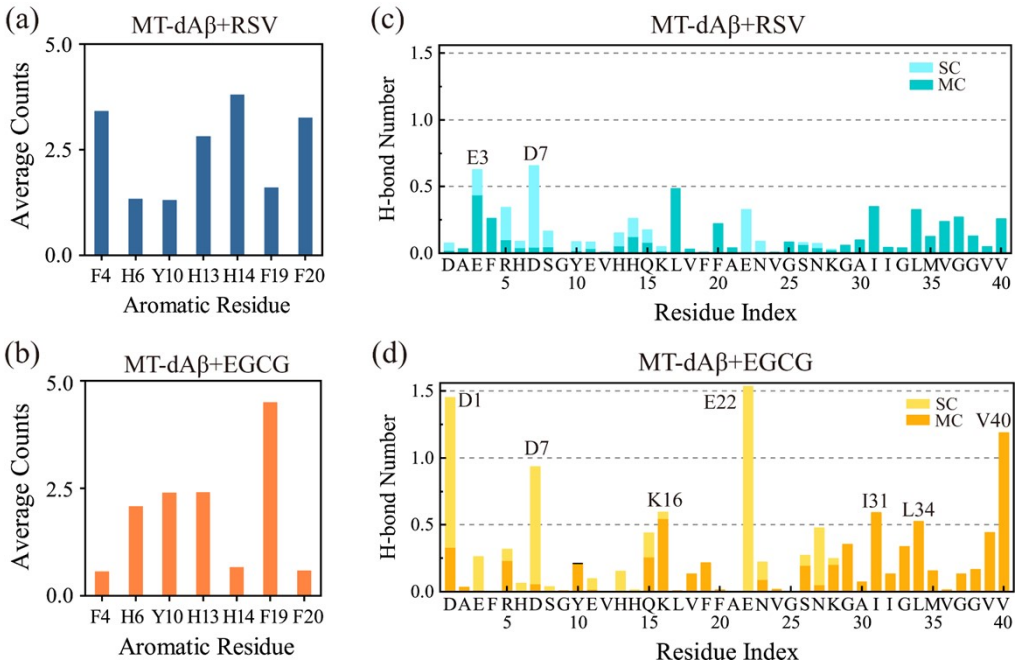

Figure S17. Comparison of aromatic and hydrogen-bonding interactions between RSV-D23N and EGCG-D23N $A\beta_{40}$ dimer. (a, b) Average π-π stacking number between (a) RSV or (b) EGCG and aromatic residues. (c, d) The main-chain (MC) and side-chain (SC) hydrogen-bond number between each residue of MT $A\beta_{40}$ and (c) RSV or (d) EGCG.

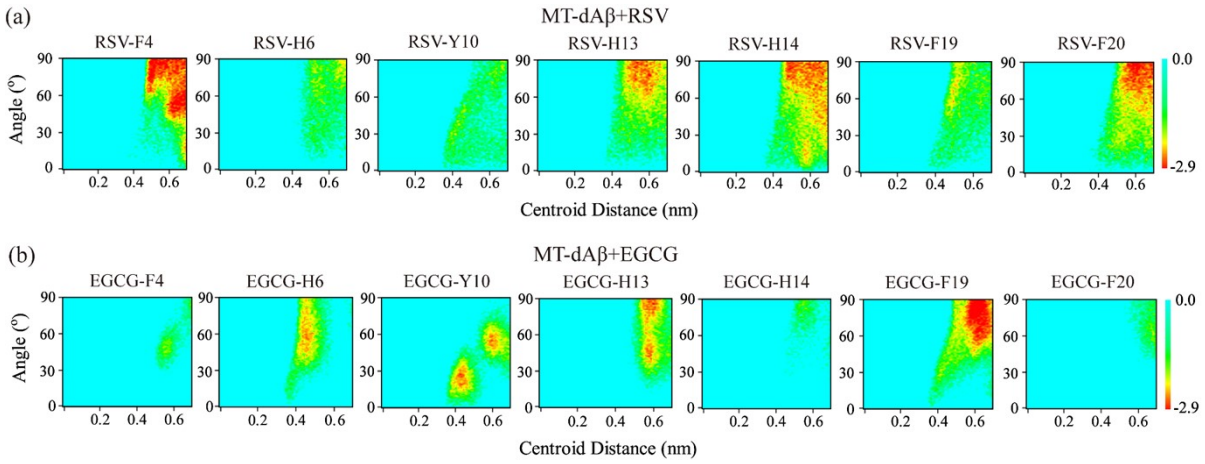

Figure S18. Potential mean force (PMF) (in kcal/mol) as a function of the centroid distance and the angle between one aromatic ring from (a) RSV or (b) EGCG and the other ring from aromatic residues in D23N MT $A\beta_{40}$.

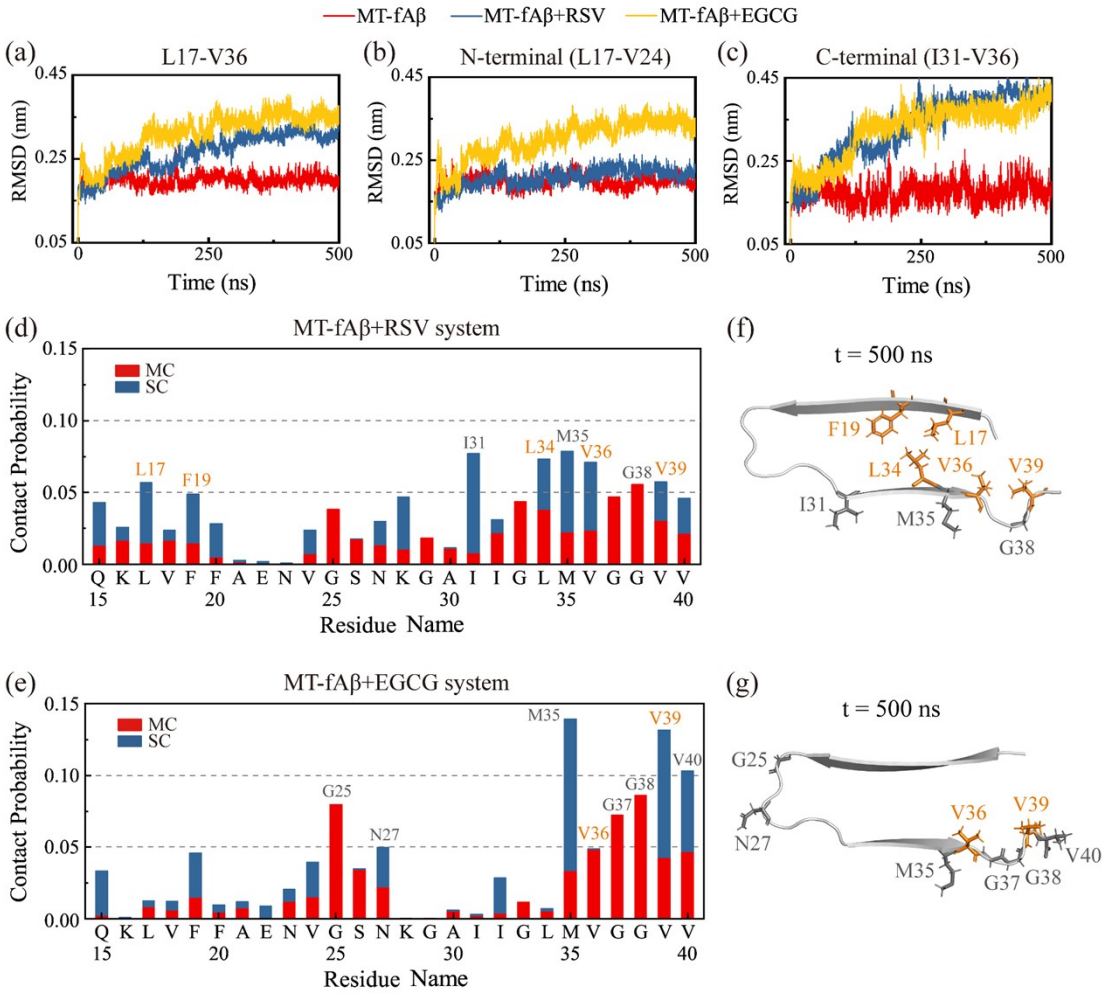

Figure S19. The influence of RSV/EGCG molecules on the structure of D23N MT $A\beta_{15-40}$ protofibril and analyses of binding sites between RSV/EGCG and the protofibril. (a-c) The time evolution of all-atom RMSD values of the L17-V36 region (a), N-terminal (L17-V24) (b), and C-terminal (I31-V36) (c) of the protofibril in MT-fAβ, MT-fAβ+RSV, and MT-fAβ+EGCG systems. When calculating the RMSD values, we exclude the random coil regions at the N-terminal and C-terminal (Q15-K16 and G37-V40). (d, e) Contact probability between RSV (d) or EGCG (e) and the MC and SC atoms of each residue. Residues having relatively high contact probabilities with RSV or EGCG are highlighted, and residues with side-chains pointing inwards are colored in orange, while those with side-chains pointing outwards are colored in gray. (f, g) A snapshot of a single chain in MT $A\beta_{15-40}$ protofibril showing the residues having high contact probabilities with RSV or EGCG. Residues with high RSV/EGCG contact probabilities are in licorice representation, residues with side-chains pointing inwards are colored in orange, and those with side-chains pointing outwards are colored in gray.

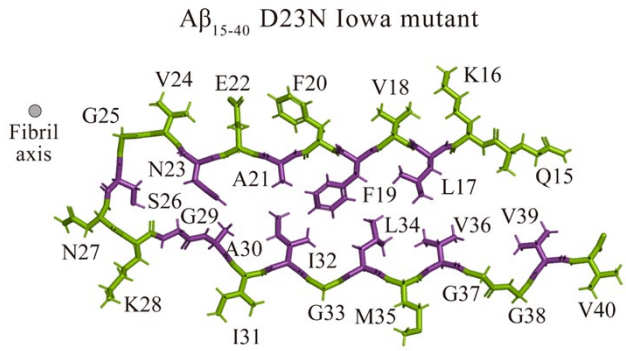

Figure S20. Structure illustration of a single chain of the D23N Iowa MT $A\beta_{15-40}$ protofibril. Residues with side-chains facing outwards are colored in green, while residues with side-chains facing inwards are colored in purple.

References

1. S. Vivekanandan, J. R. Brender, S. Y. Lee and A. Ramamoorthy, *Biochem. Biophys. Res. Commun.*, 2011, **411**, 312-316.
2. N. G. Sgourakis, W.-M. Yau and W. Qiang, *Structure*, 2015, **23**, 216-227.